

Weighted Residual Method for Solving Chemically Reacting MHD Boundary Layer Flow of Heat and Mass Transfer over a Moving Vertical Plate with Suction

^{1*}Ajala O.A., ²Oderinu R.A., ³Abimbade S.F., ⁴Aselebe L. O. and ⁵Adegoke A. O.

¹Associate Professor, Dept. of Pure and Applied Mathematics, Ladoke Akintola University of Technology, Ogbomoso, Nigeria.

²Lect. I, Dept. of Pure and Applied Mathematics, Ladoke Akintola University of Technology, Ogbomoso, Nigeria.

³M. Sc Scholar, Dept. of Statistics and Mathematical Sciences, Kwara State University, Malete, Nigeria.

^{4,5}PhD Scholar, Dept. of Pure and Applied Mathematics, Ladoke Akintola University of Technology, Ogbomoso, Nigeria.

*Corresponding Author

ABSTRACT: This study investigates the effect of chemical reaction on a free convection of a continuously moving porous vertical surface. We also studied the combined effects of wall suction and magnetic field on boundary layer flow with heat and mass transfer over an accelerating vertical plate. The governing equations of the flow which are partial differential equations were transformed into ordinary differential equations using suitable similarity transformations and the resulting coupled ordinary differential equations were solved using weighted residual method and the residuals was minimized using the collocation and partition methods . The respective collocation points were gotten using the Gauss-Laguerre Polynomial.

KEYWORDS: Magneto-Hydrodynamics, Weighted Residual Method, Partition method, Collocation method, Gauss-Laguerre Polynomial.

I. INTRODUCTION

This study investigates the interaction of conducting fluid with electromagnetic phenomena. Magnetohydrodynamic (MHD) deals with the combined effects of electromagnetic forces and fluid mechanics. It is the study of fluid that is electrically conducting such as liquid metals, plasmas and electrolytes and salt water. The fundamental concept of MHD is that the magnetic field stimulates currents in a flowing conductive fluid and causes the magnetic field to change. **Mohammad et al. (2010)** and **Xiao-hung et al, (2011)** stressed that MHD flow is of great importance in various areas of technology and engineering such as MHD power generation, MHD flow meters and MHD pumps. **Amoo et al, (2019)** stressed that in boundary layer phenomenon, radiation and chemical effects on unsteady MHD fluid flow, heat and mass transfers in porous media is significant simply because of its influence which is exponentially stretching porous surfaces. The study of unsteady MHD fluid flow has become the interest of myriads of researchers due to its broad applications in every facets of life. In recent times, many analytical and numerical studies have been conducted on MHD boundary layer flows. The free-convection flow with thermal radiation and mass transfer over a moving vertical porous plate was investigated by **Makinde (2005)**, and the effect of chemical reaction on a free convection of a continuously moving porous vertical surface was studied numerically by **Makinde and Ibrahim**

International Journal of Innovative Research in Science, Engineering and Technology

(A High Impact Factor, Monthly, Peer Reviewed Journal)

Visit: www.ijirset.com

Vol. 8, Issue 5, May 2019

(2010) using the shooting method. **Thirupathi et al, (2017)** presented finite element computation of magnetohydrodynamic nanofluid convection from an oscillating inclined plate with radiative flux, heat source and variable temperature effects. The problem of sores and radiation effects on mass transfer flow through a highly porous medium with heat generation coupled with chemical reaction was analyzed by **Shankar et al (2017)**. **Ali et al (2017)** investigated the numerical simulation of double-diffusive mixed convection in an enclosure filled with nanofluid using Bejan's heatlines and masslines. Finite element analysis of flow and heat transfer of dissipative Casson-Carreau nanofluid over a stretching sheet embedded in a porous medium was established by **Sobamowo et al (2018)**. Furthermore, many numerical studies have been made where weighted residual method was implemented. **Dada et al (2018)** stressed on the analysis of heat and mass transfer of an inclined magnetic field pressure-driven flow past a permeable plate and the transformed governing equations were solved using weighted residual method. **Anjali et al (2018)** centralized his investigation on the analysis of the effects of radiation on an MHD boundary layer flow and heat transfer over a non-linear stretching surface with variable wall temperature and non-uniform heat source/sink. **Murali et al., (2012)** studied the effect of thermal radiation on unsteady magnetohydrodynamic flow past a vertical porous plate with variable suction. **Vincent and Xiaoyun, (1994)** studied the application of weighted residual method to diffraction by 2-D canyons of arbitrary shape and consequently a solution for the two-dimensional scattering and diffraction of plane SH waves by canyons of arbitrary shape in an elastic half space was presented.

In this study, our main focus is centralized on using the weighted residual method to study effects of heat and mass transfer in a hydro magnetic boundary layer flow of a moving vertical porous plate with uniform heat generation and chemical reaction using the mathematical model presented by **Makinde and Ibrahim (2010)**.

II. MATHEMATICAL MODEL

The Continuity equation

$$\frac{\partial u}{\partial x} + \frac{\partial v}{\partial y} = 0 \quad (1)$$

The Momentum equation

$$u \frac{\partial u}{\partial x} + v \frac{\partial u}{\partial y} = V \frac{\partial^2 u}{\partial y^2} + g\beta_T(T - T_\infty) + g\beta_C(C - C_\infty) - \frac{\sigma B_0^2}{\rho} u \quad (2)$$

The Energy equation

$$u \frac{\partial T}{\partial x} + v \frac{\partial T}{\partial y} = \alpha \frac{\partial^2 T}{\partial y^2} \quad (3)$$

The Diffusivity equation

$$u \frac{\partial C}{\partial x} + v \frac{\partial C}{\partial y} = D \frac{\partial^2 C}{\partial y^2} \quad (4)$$

Where u and v are the velocity components in x and y - directions respectively. T is the temperature, β_T is the volumetric coefficient of thermal expansion, α is the thermal diffusivity, g is the acceleration due to gravity, V is the kinematic viscosity, D is the coefficient of diffusion in the mixture, C is the species concentration, σ is the electrical conductivity, B_0 is the externally imposed magnetic field in the y - direction. The relevant boundary conditions can be written as:

$$\begin{aligned} v = V, u = Bx, T = T_w = T_\infty + ax, C = C_w = C_\infty + bx, \text{ at } y=0 \\ u \rightarrow 0, T \rightarrow T_\infty, C \rightarrow C_\infty, \text{ as } y \rightarrow \infty \end{aligned} \quad (5)$$

International Journal of Innovative Research in Science, Engineering and Technology

(A High Impact Factor, Monthly, Peer Reviewed Journal)

Visit: www.ijirset.com

Vol. 8, Issue 5, May 2019

where B is a constant, a and b denotes the stratification rate of the gradient of ambient temperature and concentration profiles. We introduce the following non-dimensional variables:

$$\eta = \sqrt{\frac{B}{\nu}} y, f(\eta) = \frac{\psi}{x\sqrt{B\nu}}, \theta(\eta) = \frac{T - T_\infty}{T_w - T_\infty}, \phi(\eta) = \frac{C - C_\infty}{C_w - C_\infty} \quad (6)$$

where $f(\eta)$ is the dimensionless stream function, $\theta(\eta)$ is the dimensionless temperature of the fluid in the boundary layer region, $\phi(\eta)$ is the dimensionless species concentration of the fluid in the boundary layer region and η is the similarity variable. The velocity components u and v are respectively obtained as follows:

$$u = \frac{\partial \psi}{\partial y} = xBf'(\eta), v = -\frac{\partial \psi}{\partial x} = -\sqrt{B\nu}f(\eta) \quad (7)$$

where $f_w = \frac{V}{\sqrt{B\nu}}$ is the dimensionless suction velocity.

With this new set of independent and dependent variables defined by equation (6), the partial differential equations (2) to (4) are transformed into local similarity equations as follows:

$$f''' + ff'' - (f' + M)f' + G_T\theta + G_C\phi = 0 \quad (8)$$

$$\theta'' + \text{Pr}(f\theta' - f'\theta) = 0 \quad (9)$$

$$\phi'' + \text{Sc}(f\phi' - f'\phi) = 0 \quad (10)$$

where primes denote differentiation with respect to η . The appropriate flat plate and free convection boundary conditions are also transformed into the form:

$$\begin{aligned} f = -f_w, f' = 1, \theta = 1, \phi = 1, \quad \text{at } \eta = 0 \\ f' = 0, \theta = 0, \phi = 0, \quad \text{as } \eta \rightarrow \infty \end{aligned} \quad (11)$$

where

$$M = \frac{\sigma B_0^2}{\rho B} \text{ is the magnetic parameter,}$$

$$\text{Pr} = \frac{\nu}{\alpha} \text{ is the Prandtl number,}$$

$$\text{Sc} = \frac{\nu}{D} \text{ is the Schmidt number,}$$

$$G_T = \frac{g\beta_T(T_w - T_\infty)}{xB^2} \text{ is the local temperature Grashof number,}$$

$$G_C = \frac{g\beta_C(C_w - C_\infty)}{xB^2} \text{ is the local concentration Grashof number.}$$

International Journal of Innovative Research in Science, Engineering and Technology

(A High Impact Factor, Monthly, Peer Reviewed Journal)

Visit: www.ijirset.com

Vol. 8, Issue 5, May 2019

III. GAUSS – LAGUERRE POLYNOMIAL

$$L_n(x) = e^x \frac{d^n}{dx^n} (e^{-x} x^n)$$

N	Roots (x_i)	Weights (A_i)
8	0.170279632	0.36918859
	0.903701777	0.41876678
	2.251086630	0.17579497
	4.266700170	0.03334349
	7.045905402	0.00279454
	10.75851601	0.00009077
	15.74067864	8.4857E(-7)
	22.86313174	1.0480E(-9)

IV. THE PRINCIPLE OF WEIGHTED RESIDUAL METHOD (WRM)

STEP 1: We assume the trial functions which are solutions for the system of equations to be solved.

STEP 2: We obtain the residual function by substituting the trial function into the system of equations to be solved:

STEP 3: We impose the corresponding boundary conditions on the trial functions and minimise the residual (using the partition and collocation method):

STEP 4: We solve for the unknowns.

V. NUMERICAL PROCEDURE

Partition method

STEP 1: $F = \sum_{i=0}^{10} a_i e^{\frac{-i}{4}x}, \theta = \sum_{i=0}^{10} b_i e^{\frac{-i}{4}x}, \phi = \sum_{i=0}^{10} c_i e^{\frac{-i}{4}x}$

STEP 2:

$$fr = \left(\sum_{i=0}^{10} a_i e^{\frac{-i}{4}x} \right)''' + \left(\sum_{i=0}^{10} a_i e^{\frac{-i}{4}x} \right) \left(\sum_{i=0}^{10} a_i e^{\frac{-i}{4}x} \right)'' - \left(\left(\sum_{i=0}^{10} a_i e^{\frac{-i}{4}x} \right)' + M \right) \left(\sum_{i=0}^{10} a_i e^{\frac{-i}{4}x} \right)' + G_T \sum_{i=0}^{10} b_i e^{\frac{-i}{4}x}$$

$$\theta r = \left(\sum_{i=0}^{10} b_i e^{\frac{-i}{4}x} \right)'' + Pr \left(\left(\sum_{i=0}^{10} a_i e^{\frac{-i}{4}x} \right) \left(\sum_{i=0}^{10} b_i e^{\frac{-i}{4}x} \right)' - \left(\sum_{i=0}^{10} a_i e^{\frac{-i}{4}x} \right)' \left(\sum_{i=0}^{10} b_i e^{\frac{-i}{4}x} \right) \right)$$

$$\phi r = \left(\sum_{i=0}^{10} c_i e^{\frac{-i}{4}x} \right)'' + Sc \left(\left(\sum_{i=0}^{10} c_i e^{\frac{-i}{4}x} \right) \left(\sum_{i=0}^{10} c_i e^{\frac{-i}{4}x} \right)' - \left(\sum_{i=0}^{10} a_i e^{\frac{-i}{4}x} \right)' \left(\sum_{i=0}^{10} c_i e^{\frac{-i}{4}x} \right) \right)$$

STEP 3:

$$eq1 = f(x=0) + f_w, \quad eq2 = f'(x=0) - 1, \quad eq3 = \theta(x=0) - 1, \quad eq4 = \phi(x=0) - 1,$$

$$eq5 = f'(x=\infty), \quad eq6 = \theta(x=\infty), \quad eq7 = \phi(x=\infty)$$

We then minimize the residual function. Here, the entire domain R is divided into n non overlapping sub domains R_j where $j = 1, 2, \dots, n$. If the weighing functions are chosen as

International Journal of Innovative Research in Science, Engineering and Technology

(A High Impact Factor, Monthly, Peer Reviewed Journal)

Visit: www.ijirset.com

Vol. 8, Issue 5, May 2019

$$f_j = 1 \quad \text{If } x \in R_j, \quad f_j = 0 \quad \text{If } x \notin R_j$$

Then the required equation of partitions becomes

$$\int_{R_j} E(x, a) dx = 0 \quad j = 1, 2, \dots, n$$

Therefore in the light of this, we integrate the residual functions using the interval of 1 so that the residual will be minimized more accurately. Furthermore, we supply the numeric values of our parameters (Pr, M, G_T, G_C, f_w) . Finally, we obtain the solutions for F, θ, ϕ by evaluating the trial functions at the points $(a_0 \dots a_{10})$, $(b_0 \dots b_{10})$ and $(c_0 \dots c_{10})$ respectively.

Collocation method

$$\text{STEP 1: } f = \sum_{i=0}^9 a_i e^{\frac{-i}{5}x}, \theta = \sum_{i=0}^9 b_i e^{\frac{-i}{5}x}, \phi = \sum_{i=0}^9 c_i e^{\frac{-i}{5}x}$$

$$\text{STEP 2: } fr = \left(\sum_{i=0}^9 a_i e^{\frac{-i}{5}x} \right)''' + \left(\sum_{i=0}^9 a_i e^{\frac{-i}{5}x} \right) \left(\sum_{i=0}^9 a_i e^{\frac{-i}{5}x} \right)'' - \left(\left(\sum_{i=0}^9 a_i e^{\frac{-i}{5}x} \right)' + M \right) \left(\sum_{i=0}^9 a_i e^{\frac{-i}{5}x} \right)' + G_T \sum_{i=0}^9 b_i e^{\frac{-i}{5}x}$$

$$\theta r = \left(\sum_{i=0}^9 b_i e^{\frac{-i}{5}x} \right)'' + Pr \left(\left(\sum_{i=0}^9 a_i e^{\frac{-i}{5}x} \right) \left(\sum_{i=0}^9 b_i e^{\frac{-i}{5}x} \right)' - \left(\sum_{i=0}^9 a_i e^{\frac{-i}{5}x} \right)' \left(\sum_{i=0}^9 b_i e^{\frac{-i}{5}x} \right) \right)$$

$$\phi r = \left(\sum_{i=0}^9 c_i e^{\frac{-i}{5}x} \right)'' + Sc \left(\left(\sum_{i=0}^9 c_i e^{\frac{-i}{5}x} \right) \left(\sum_{i=0}^9 c_i e^{\frac{-i}{5}x} \right)' - \left(\sum_{i=0}^9 a_i e^{\frac{-i}{5}x} \right)' \left(\sum_{i=0}^9 c_i e^{\frac{-i}{5}x} \right) \right)$$

STEP 3:

$$eq1 = f(x=0) + f_w, eq2 = f'(x=0) - 1, eq3 = \theta(x=0) - 1, eq4 = \phi(x=0) - 1, \\ eq5 = f'(x=\infty), eq6 = \theta(x=\infty), eq7 = \phi(x=\infty)$$

We then minimize the residual function. Here, we choose n points $x_1, x_2 \dots x_n$ in the domain R and define the weighting function as $f_j = \delta(x - x_j)$ where δ represents the unit impulse or Dirac delta which vanishes everywhere except at $x = x_j$. The collocation equation becomes $\int \delta(x - x_j) E(x, a) dx = 0$. This is equivalent to putting $E(x, a)$ equal to zero at n points in the domain R . Here, we chose the collocation points using the Laguerre Polynomial.

International Journal of Innovative Research in Science, Engineering and Technology

(A High Impact Factor, Monthly, Peer Reviewed Journal)

Visit: www.ijirset.com

Vol. 8, Issue 5, May 2019

VI. RESULTS AND DISCUSSIONS

Partition method

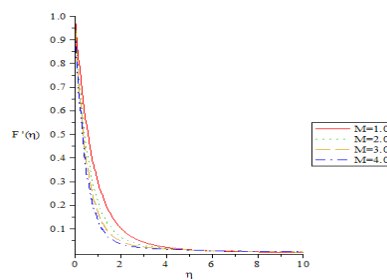


Figure 1: Velocity profiles for $Pr = 0.72,$
 $Sc = 0.62, f_w = G_T = G_C = .1$

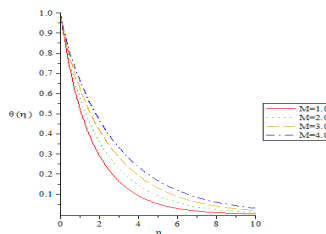


Figure 2: Temperature profiles for $Pr = 0.72,$
 $Sc = 0.62, f_w = G_T = G_C = .1$

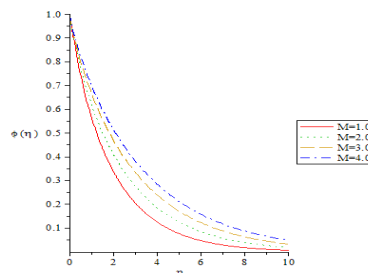


Figure 3:
Concentration profiles for $Pr = 0.72,$
 $Sc = 0.62, f_w = G_T = G_C = .1$

International Journal of Innovative Research in Science, Engineering and Technology

(A High Impact Factor, Monthly, Peer Reviewed Journal)

Visit: www.ijirset.com

Vol. 8, Issue 5, May 2019

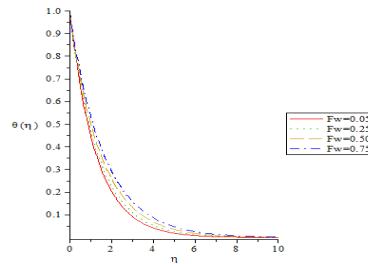


Figure 4: Velocity profiles for $Pr=0.72$, $Sc=0.62$, $M=G_T=G_c=0.1$

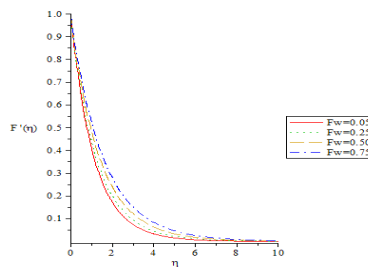


Figure 5: Temperature profiles for $Pr=0.72$, $Sc=0.62$,
 $M=G_T=G_c=0.1$

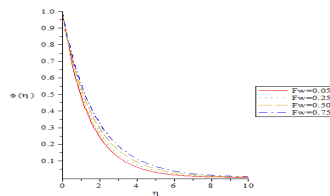


Figure 6: Concentration profiles for $Pr=0.72$, $Sc=0.62$, $M=G_T=G_c=0.1$

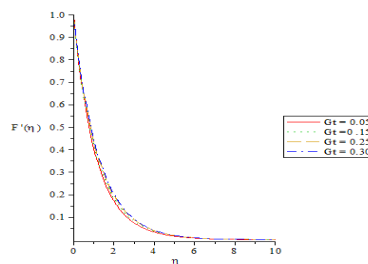


Figure 7: Velocity profiles for $Pr = 0.72$,
 $Sc = 0.62, M = f_w = G_c = 0.1$

International Journal of Innovative Research in Science, Engineering and Technology

(A High Impact Factor, Monthly, Peer Reviewed Journal)

Visit: www.ijirset.com

Vol. 8, Issue 5, May 2019

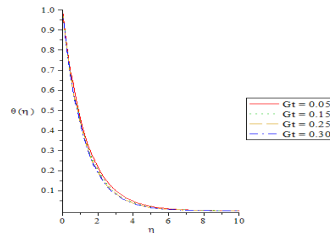


Figure 8: Temperature profiles for $Pr = 0.72$,
 $Sc = 0.62, M = f_w = G_c = 0.1$

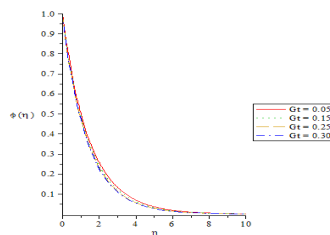


Figure 9:
 $Pr = 0.72$,
Concentration profiles for $Sc = 0.62, M = f_w = G_c = 0.1$

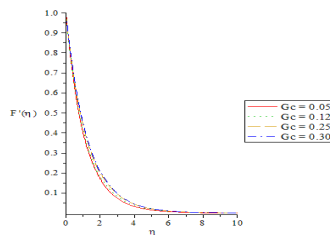


Figure 10: Velocity profiles for $Pr = 0.72$,
 $Sc = 0.62, M = f_w = G_T = 0.1$

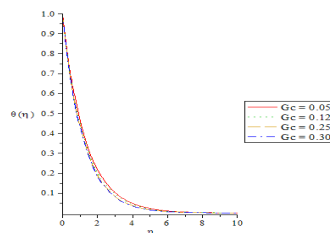


Figure 11:
 $Pr = 0.72$,
Temperature profiles for $Sc = 0.62, M = f_w = G_T = 0.1$

International Journal of Innovative Research in Science, Engineering and Technology

(A High Impact Factor, Monthly, Peer Reviewed Journal)

Visit: www.ijirset.com

Vol. 8, Issue 5, May 2019

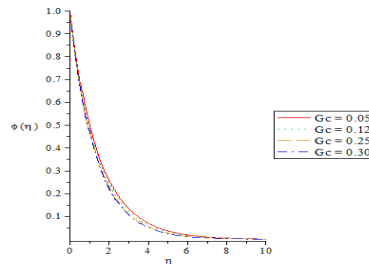


Figure 12:
Pr = 0.72,
Concentration profiles for $Sc = 0.62, M = f_w = G_T = 0.1$

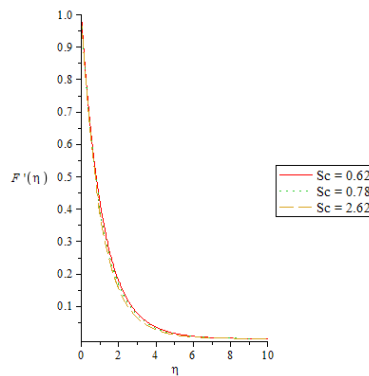


Figure 13: Velocity profiles for Pr=0.72, Sc=0.62, M=f_w=G_T=G_c=0.1

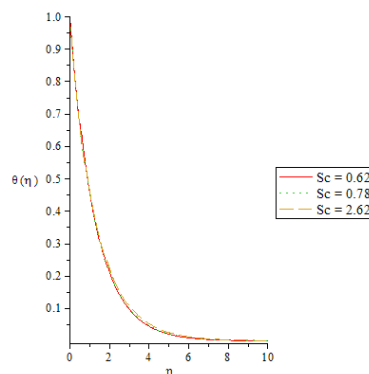


Figure 14: Temperature profiles for Pr=0.72, Sc=0.62, M=f_w=G_T=G_c=0.1

International Journal of Innovative Research in Science, Engineering and Technology

(A High Impact Factor, Monthly, Peer Reviewed Journal)

Visit: www.ijirset.com

Vol. 8, Issue 5, May 2019

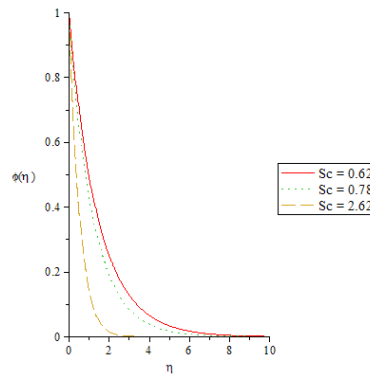


Figure 15: Concentration profiles for $Pr=0.72$, $Sc=0.62$, $M=f_w=G_T=G_c=0.1$

Collocation method

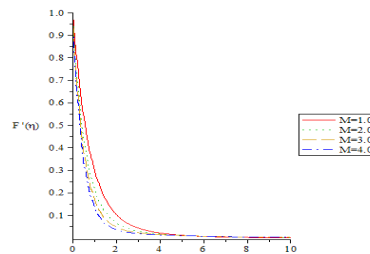


Figure 16: Velocity profiles for $Pr = 0.72$,
 $Sc = 0.62$, $f_w = G_T = G_C = .1$

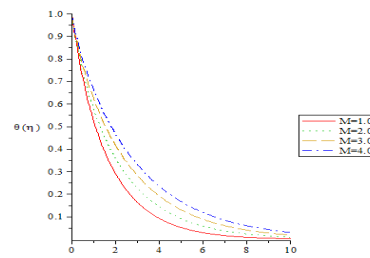


Figure 17:
Temperature profiles for
 $Pr = 0.72$,
 $Sc = 0.62$, $f_w = G_T = G_C = 0.1$

International Journal of Innovative Research in Science, Engineering and Technology

(A High Impact Factor, Monthly, Peer Reviewed Journal)

Visit: www.ijirset.com

Vol. 8, Issue 5, May 2019

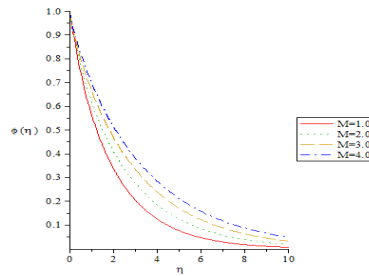


Figure 18: Concentration profiles for $Pr = 0.72,$
 $Sc = 0.62, f_w = G_T = G_C = 0.1$

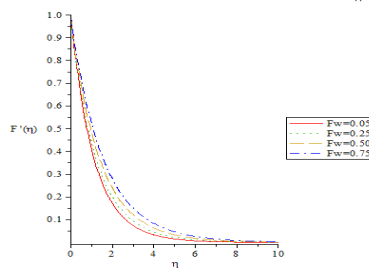


Figure 19:
 $Pr = 0.72,$
Velocity profiles for $Sc = 0.62, M = G_T = G_C = 0.1$

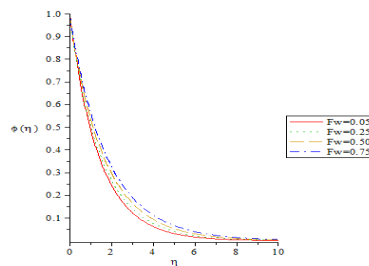


Figure 20: Concentration profiles for $Pr = 0.72,$
 $Sc = 0.62, M = G_T = G_C = 0.1$

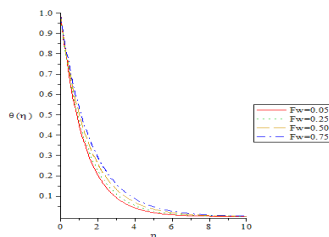


Figure 21:
 $Pr = 0.72,$
Temperature profiles for $Sc = 0.62, M = G_T = G_C = 0.1$

International Journal of Innovative Research in Science, Engineering and Technology

(A High Impact Factor, Monthly, Peer Reviewed Journal)

Visit: www.ijirset.com

Vol. 8, Issue 5, May 2019

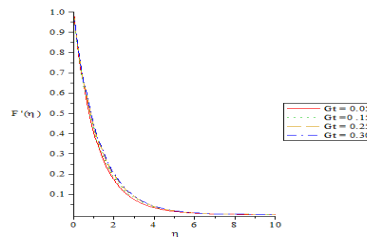


Figure 22:
Pr = 0.72,
Velocity profiles for $Sc = 0.62, M = f_w = G_C = 0.1$

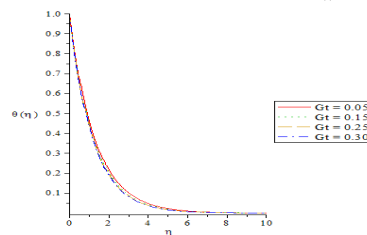


Figure 23:
Pr = 0.72,
Temperature profiles for $Sc = 0.62, M = f_w = G_C = 0.1$

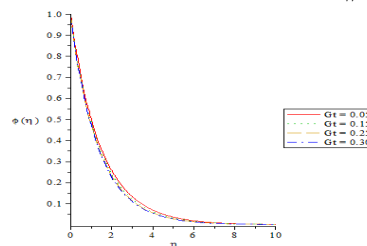


Figure 24:
Pr = 0.72,
Concentration profiles for $Sc = 0.62, M = f_w = G_C = 0.1$

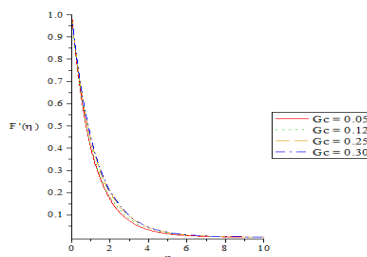


Figure 25:
Pr = 0.72,
Velocity profiles for $Sc = 0.62, M = f_w = G_T = 0.1$

International Journal of Innovative Research in Science, Engineering and Technology

(A High Impact Factor, Monthly, Peer Reviewed Journal)

Visit: www.ijirset.com

Vol. 8, Issue 5, May 2019

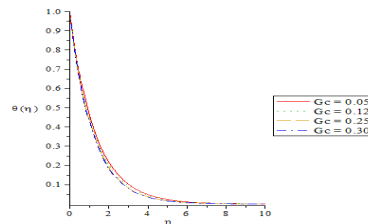


Figure 26:
Pr = 0.72,
Temperature profiles for
 $Sc = 0.62, M = f_w = G_T = 0.1$

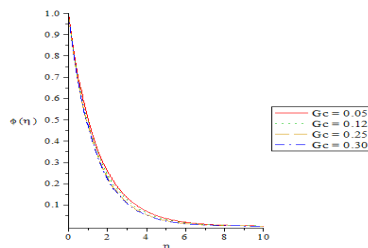


Figure 27:
Pr = 0.72,
Concentration profiles for
 $Sc = 0.62, M = f_w = G_T = 0.1$

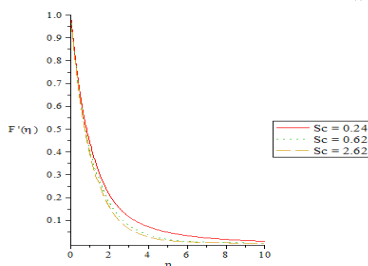


Figure 28:
Pr = 0.72,
Velocity profiles for
 $M = f_w = G_T = G_C = 0.1$

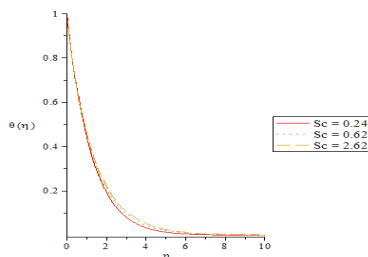


Figure 29:
Pr = 0.72,
Temperature profiles for
 $M = f_w = G_T = G_C = 0.1$

International Journal of Innovative Research in Science, Engineering and Technology

(A High Impact Factor, Monthly, Peer Reviewed Journal)

Visit: www.ijirset.com

Vol. 8, Issue 5, May 2019

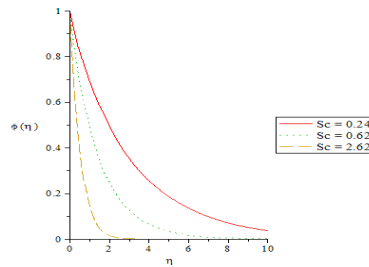


Figure 30:
Pr = 0.72,
Concentration profiles for $M = f_w = G_t = G_c = 0.1$

Computation showing $f''(0)$, $-\theta'(0)$ and $-\phi'(0)$ for various parameters when Pr = 0.72

TABLE 1: Partition method

M	Fw	Gt	Gc	Sc	$f''(0)$	$-\theta'(0)$	$-\phi'(0)$
1.0	0.1	0.1	0.1	0.62	1.264451	0.708491	0.640005
2.0	0.1	0.1	0.1	0.62	1.592592	0.638163	0.574501
3.0	0.1	0.1	0.1	0.62	1.868425	0.585920	0.525473
4.0	0.1	0.1	0.1	0.62	2.110581	0.544220	0.484910
0.1	0.05	0.1	0.1	0.62	0.912189	0.812883	0.738697
0.1	0.25	0.1	0.1	0.62	0.822914	0.749729	0.686120
0.1	0.50	0.1	0.1	0.62	0.725057	0.678487	0.626724
0.1	0.75	0.1	0.1	0.62	0.641343	0.615183	0.573946
0.1	0.1	0.05	0.1	0.62	0.914698	0.789900	0.718508
0.1	0.1	0.15	0.1	0.62	0.863624	0.802753	0.731248
0.1	0.1	0.25	0.1	0.62	0.814217	0.814053	0.742399
0.1	0.1	0.30	0.1	0.62	0.790024	0.819265	0.747525
0.1	0.1	0.1	0.05	0.62	0.916268	0.788847	0.717393
0.1	0.1	0.1	0.12	0.62	0.878169	0.799444	0.727997
0.1	0.1	0.1	0.25	0.62	0.810311	0.816186	0.744642
0.1	0.1	0.1	0.30	0.62	0.784989	0.821915	0.750306
0.1	0.1	0.1	0.1	0.62	0.888923	0.796559	0.725115
0.1	0.1	0.1	0.1	0.78	0.893471	0.793681	0.834028
0.1	0.1	0.1	0.1	2.62	0.912542	0.784714	1.644608

International Journal of Innovative Research in Science, Engineering and Technology

(A High Impact Factor, Monthly, Peer Reviewed Journal)

Visit: www.ijirset.com

Vol. 8, Issue 5, May 2019

TABLE 2: Collocation method

M	Fw	Gt	Gc	Sc	$f''(0)$	$-\theta'(0)$	$-\phi'(0)$
1.0	0.1	0.1	0.1	0.62	1.264472	0.708916	0.639962
2.0	0.1	0.1	0.1	0.62	1.592395	0.637229	0.571256
3.0	0.1	0.1	0.1	0.62	1.868084	0.582067	0.518819
4.0	0.1	0.1	0.1	0.62	2.110052	0.537591	0.476899
0.1	0.05	0.1	0.1	0.62	0.912211	0.812864	0.738855
0.1	0.25	0.1	0.1	0.62	0.823027	0.749800	0.686483
0.1	0.50	0.1	0.1	0.62	0.725347	0.678809	0.627324
0.1	0.75	0.1	0.1	0.62	0.641782	0.615851	0.574487
0.1	0.1	0.05	0.1	0.62	0.914765	0.789928	0.718772
0.1	0.1	0.15	0.1	0.62	0.863638	0.802725	0.731399
0.1	0.1	0.25	0.1	0.62	0.814195	0.814000	0.742468
0.1	0.1	0.30	0.1	0.62	0.789993	0.819206	0.747564
0.1	0.1	0.1	0.05	0.62	0.916309	0.788874	0.717664
0.1	0.1	0.1	0.12	0.62	0.878206	0.799430	0.728176
0.1	0.1	0.1	0.25	0.62	0.810318	0.816142	0.744696
0.1	0.1	0.1	0.30	0.62	0.784985	0.821867	0.750326
0.1	0.1	0.1	0.1	0.24	0.868964	0.810803	0.398212
0.1	0.1	0.1	0.1	0.62	0.888962	0.796554	0.796554
0.1	0.1	0.1	0.1	2.62	0.912302	0.784763	1.648001

Analysis of results

Numerical results are reported in the Tables 1 to 2 and Figures 1 to 30. The Prandtl number was taken to be $Pr = 0.72$, which corresponds to air, the values of Schmidt number (Sc) were chosen to be $Sc = 0.24, 0.62, 0.78, 2.62$, representing diffusing chemical species of most common interest in air like H_2, H_2O, NH_3 and Propyl Benzene, respectively. Attention is focused on positive values of the buoyancy parameters, that is, Grashof number $G_T > 0$ (which corresponds to the cooling problem) and solutal Grashof number $G_C > 0$ (which indicates that the chemical species concentration in the free stream region is less than the concentration at the boundary surface) Makinde and Ibrahim (2010).

From Table 1 and 2, we discovered that an increase in the magnetic field intensity will cause a decrease in the heat and mass rate at the surface and an increase in the skin friction. Also, an increase in the magnitude of the fluid suction will cause a decrease in the skin friction and also in the heat and mass transfer rate at the surface. Furthermore, an increase in the intensity of the buoyancy force will cause an increase in the heat and mass transfer rate and a decrease in the skin friction. Finally, an increase in the Schmidt number (Sc) will cause an increase in the skin friction and the surface mass transfer rate while a decrease in the surface heat transfer rate will be noticed.

As shown in Figures 1 to 3 and Figures 16 to 18, an increase in the magnetic field intensity will cause a decrease in the fluid velocity and an increase in the fluid temperature and the chemical species concentration. Figures 4 to 6 and Figures 19 to 21 explains that as magnitude of the fluid suction increases, there will be an all-round increase in the fluid velocity, fluid temperature and chemical species concentration. Also, as shown in figures 7 to 12 and figures 22 to 27, an increase in the buoyancy forces will cause an increase in the fluid velocity, and a decrease in the heat and mass transfer rate. Finally, an increase in the Schmidt number will cause an increase in the heat transfer rate and a decrease in the fluid velocity and mass transfer rate.

International Journal of Innovative Research in Science, Engineering and Technology

(A High Impact Factor, Monthly, Peer Reviewed Journal)

Visit: www.ijirset.com

Vol. 8, Issue 5, May 2019

VII. CONCLUSIONS

This paper reviewed the work of Makinde and Ibrahim 2010 using the method of weighted residuals and the residual was minimised using the partition and the collocation methods. It studied the combined effects of wall suction and magnetic field on boundary layer flow with heat and mass transfer over an accelerating vertical plate. The result was duly interpreted and discussed and it was inferred that the momentum boundary layer thickness decreases, while both thermal and concentration boundary layer thicknesses increases with an increase in the magnetic field intensity. Furthermore, an increase in wall suction enhances the boundary layer thickness and reduces the skin friction together with the heat and mass transfer rate at the moving plate surface.

REFERENCES

- [1] Amoo S. A., Adamu A. K. and Henry O., "Radiation and Radiation effects on Unsteady Magnetohydrodynamics Boundary Layer Fluid Flow in Porous Media", Journal of Science and Technology Research 1(1), Pp. 113-121, 2019.
- [2] Ali Akbar A. A., Ahmad Ababaci, Ghanbar A. S and Alireza A., "Numerical simulation of double diffusive mixed convection in an enclosure filled with nanofluid using Bejan's heatlines and masslines", Alexandria Engineering journal, 2017, www.sciencedirect.com.
- [3] Anjali Devi S. P., Agneeshwari M and Wilfred Raj J. S., "Radiation effects on MHD boundary layer flow and heat transfer over a non-linear stretching surface with variable wall temperature and non-uniform heat source/sink", Intl' Journal of Applied Mechanics and Engineering, Vol. 23, No. 2. Pp. 289-305, 2018.
- [4] Dada M. S and Salawu S. O., "Analysis of heat and mass transfer of an inclined magnetic field pressure-driven flow past a permeable plate", Applications and Applied Mathematics, an Intl' Journal, Vol. 12. Pp. 189-200, 2018.
- [5] Makinde O.D., "Free-convection flow with thermal radiation and mass transfer past a moving vertical porous plate", Int. Communication. Heat mass transfer, 32(10): 1411-1419, 2005.
- [6] Makinde O.D., "Effect of arbitrary magnetic Reynolds number on MHD flows in convergent-divergent channel", Int. J. Num. Meth. Heat fluid flow, 18(6): 697-707, 2008.
- [7] Makinde O.D., "On MHD boundary-layer flow and mass transfer past a vertical plate in a porous medium with constant heat flux", Int. J. Num. Meth. Heat fluid flow, 19(34): 546-554, 2009.
- [8] Makinde O.D. and Ibrahim S.Y., "Chemically reacting MHD boundary layer flow of heat and mass transfer over a moving vertical plate with suction", Scientific Research and Essay, 5(19): 2875-2882, 2010.
- [9] Mohammad Mehdi Rashidi and Mohammad Keimanesh, "Using Differential Transform method and Pade Approximant for solving MHD flow in a laminar liquid film from Horizontal Stretching Surface", Mathematical problems in Engineering, Article ID 491319 doi:10.1155/2010/491319, 2010.
- [10] Murali Gundagani, Sivaiah S., Babu N. V. N and M. C. K., Reddy, "Finite element solution of thermal radiation effect on unsteady MHD flow past a vertical porous plate with variable suction", American Academic and Scholarly Research Journal, Vol. 4, No. 3, 2012. www.aasrc.org/aasrj.
- [11] Shankar Goud .B and Raja Shekar M. N., "Finite element study of sores and radiation effects on mass transfer flow through a highly porous medium with heat generation and chemical reaction", Intl' Journal of Computational and Applied Mathematics. Vol. 12, No. 1, Pp. 53-64, 2017.
- [12] Sobamowo M.G, Yinusa A.A, Oluwo A.A and Alozie S. I., "Finite element analysis of flow and heat transfer of dissipative Casson-Carreau nanofluid over a stretching sheet embedded in a porous medium", Aeronautics and Aerospace Open Access Journal, Vol., 2, Issue 5-2018.
- [13] Thirupathi Thumma, O. Anwar Beg and Siva Reddy Sheri, "Finite Element Computation of Magnetohydrodynamic Nanofluid Convection from an Oscillating Inclined Plate with Radiative Flux, Heat Source and Variable Temperature Effects. Proc imeche-part n-journal of nanomaterials nanoengineering and nanosystems", 2017.
- [14] Vincent W. Lee and Xiaoyun Wu, "Application of the weighted residual method to diffraction by 2-D canyons of arbitrary shape: I. Incident SH waves", Int. J. Soil Dynam. and earthq. Engng, , 0267-726 94/50700, 1994.
- [15] Xiao-hong Su and Lian-cun Zheng, "Approximate solution to MHD Falkner-Skan flow over permeable wall", Appl. Math. Mech-Engl.Ed, vol. 32 no. 4: 401-408, 2011.